Saudi Journal of Biological Sciences 27 (2020) 1080–1090

Contents lists available at ScienceDirect

Saudi Journal of Biological Sciences

journal homepage: www.sciencedirect.com

Original article

Food color 'Azorubine' interferes with quorum sensing regulated functions and obliterates biofilm formed by food associated bacteria: An *in vitro* and *in silico* approach

Nasser A. Al-Shabib [a,*], Fohad Mabood Husain [a,*], Md Tabish Rehman [b], Abdullah A. Alyousef [c], Mohammed Arshad [c], Altaf Khan [d], Javed Masood Khan [a], Pravej Alam [e], Thamer A. Albalawi [e], Syed Ali Shahzad [a], Jakeera B. Syed [f], Mohamed F. Al-ajmi [b]

[a] Department of Food Science and Nutrition, Faculty of Food and Agricultural Sciences, King Saud University, 2456, Riyadh 11451, Saudi Arabia
[b] Department of Pharmacognosy, College of Pharmacy, King Saud University, 2460, Riyadh 11451, Saudi Arabia
[c] Department of Clinical Laboratory Sciences, College of Applied Medical Sciences, King Saud University, 2460, Riyadh 11451, Saudi Arabia
[d] Department of Pharmacology and Toxicology, Central Laboratory, College of Pharmacy, King Saud University, 2460, Riyadh 11451, Saudi Arabia
[e] Department of Biology, Prince Sattam bin Abdulaziz Univrsity, Alkharj, Saudi Arabia
[f] College of Medicine and Dentistry, Dar Al Uloom University, Al Mizan St, Al Falah, Riyadh 13314, Saudi Arabia

ARTICLE INFO

Article history:
Received 17 September 2019
Revised 16 December 2019
Accepted 6 January 2020
Available online 16 January 2020

Keywords:
Azorubine
Quorum sensing
Biofilm
Virulence
Food
Molecular docking

ABSTRACT

Quorum sensing (QS) plays a crucial role in different stages of biofilm development, virulence production, and subsequently to the growth of bacteria in food environments. Biofilm mediated spoilage of food is one of the ongoing challenge faced by the food industry worldwide as it incurs substantial economic losses and leads to various health issues. In the present investigation, we studied the interference of quorum sensing, its regulated virulence functions, and biofilm in food-associated bacteria by colorant azorubine. *In vitro* bioassays demonstrated significant inhibition of QS and its coordinated virulence functions in *Chromobacterium violaceum* 12472 (violacein) and *Pseudomonas aeruginosa* PAO1 (elastase, protease, pyocyanin, and alginate). Further, the decrease in the production EPS (49–63%) and swarming motility (61–83%) of the pathogens was also recorded at sub-MICs. Azorubine demonstrated broad-spectrum biofilm inhibitory potency (50–65%) against *Chromobacterium violaceum*, *Pseudomonas aeruginosa*, *E. coli* O157:H7, *Serratia marcescens*, and *Listeria monocytogenes*. ROS generation due to the interaction between bacteria and azorubine could be responsible for the biofilm inhibitory action of the food colorant. Findings of the *in vitro* studies were well supported by molecular docking and simulation analysis of azorubine and QS virulence proteins. Azorubine showed strong binding to PqsA as compared to other virulent proteins (LasR, Vfr, and QscR). Thus, it is concluded that azorubine is a promising candidate to ensure food safety by curbing the menace of bacterial QS and biofilm-based spoilage of food and reduce economic losses.

1. Introduction

Food-borne bacteria mediated spoilage of food is one of the ongoing challenge faced by the food industry worldwide. The problem does not only lead to substantial economical losses due to excessive food deterioration but also poses grave health care related issues, with severe risk of the outbreak of acute diseases (Skandamis and Nychas, 2012). Interestingly, majority of the food-borne pathogens are capable of forming biofilm, a sessile bacterial community embedded in a self-produced protective matrix (Parsek and Greenberg, 2005; Solano et al., 2014). These complex three-dimensional structures protect the bacteria from harsh external

* Corresponding authors.
E-mail addresses: nalshabib@ksu.edu.sa (N.A. Al-Shabib), fhusain@ksu.edu.sa (F.M. Husain).

Peer review under responsibility of King Saud University.

Production and hosting by Elsevier

https://doi.org/10.1016/j.sjbs.2020.01.001
1319-562X/

environments, provide better availability of nutrients, and organize genetic diversity of the community (Johnson, 2008). Once established on food surfaces or in processing environments, biofilms are tough to remove and are highly resistant to cleansing agents including most of the commonly used antibiotics (Høiby et al., 2010). Increased antibiotic resistance to biofilms could be related to several mechanisms including formation of tough physical barriers as a result of increased extracellular polymeric substances (EPS) secretion, upregulation of specific resistance genes which are unique to biofilms and alteration of metabolic activity (Jw et al., 1999; Mah and O'Toole, 2001; Nguyen et al., 2011). These specialized features of bacterial biofilms create resistance to antimicrobial agents and thus need novel strategies that effectively eradicate the bacterial biofilms.

Quorum sensing, a global regulatory network, characterized in majority of bacteria including biofilm forming food-borne pathogens, involves the production of extracellular small signaling molecules or autoinducers (AIs). Subsequent detection of which induces expression of certain specific genes as a function of increasing bacterial population density (Bai and Rai, 2011; Rutherford et al., 2014). Recent developments have shown that quorum sensing (QS) plays a crucial role in one or more stage of biofilm development, virulence production and subsequently to the growth of bacteria in food environments (Khan et al., 2017). Thus, disruption of bacterial communication system offers an alternative and possibly safer strategy for effectively controlling biofilm mediated food spoilage and illness. Targeting QS is strategically advantageous over conventional antibacterials, as the former does not involve the suppression of bacterial growth and hence will not exert selective pressure leading to the development of resistance (LaSarre and Federle, 2013). In this context, researchers are exploring various compounds as potential quorum sensing inhibitors (QSIs) in the food industry.

Food colors are a class of food additives that have been used extensively to provide color to a variety of food, drugs, and cosmetics. Food colors significantly enhance the appeal of the food items and make them more lucrative for the consumers (Hallagan et al., 1995). Food colorants are both natural and synthetic, and one such artificial color is a red azo dye called Azorubine. It is a disodium salt, red to maroon in color, highly water soluble and used in food items that are heat-treated after fermentation. Azorubine is present in food items like swiss rolls, jellies, jams, yoghurts, cheesecakes mixes and bread crumbs etc. It is also a constituent of mouth wash (Amin et al., 2010). Azorubine is reported to have antioxidant activity (Obón et al., 2005) and is also observed to bind with DNA (Basu and Kumar, 2014) and essential proteins like human serum albumin, bovine serum albumin and Haemoglobin (Basu and Suresh Kumar, 2014; Basu and Suresh Kumar, 2015). However, still, there is a scope to assess the quorum quenching and biofilm inhibitory property of this colorant against pathogenic bacteria.

Therefore, in the current study, we have studied the interference of quorum sensing and its regulated virulence functions in food-associated bacteria by azorubine. Additionally, we undertook the elucidation of inhibitory action of the colorant against bacterial biofilms and factors that contribute to biofilm formation. Molecular docking and simulation studies with QS proteins were also performed to ascertain the findings of *in vitro* studies.

2. Materials and methods

2.1. Materials

Azorubine was purchased from Sigma Aldrich, USA. TTC (2,3,5-triphenyl tetrazolium chloride) and Crystal violet were acquired from HiMedia laboratories, Mumbai, India. All organic solvents used in the current investigation were procured from Sigma Aldrich, USA.

2.2. Bacterial strains

Gram positive and Gram negative food-associated bacteria were used in the present study. *Chromobacterium violaceum* (ATCC 12472), *Pseudomonas aeruginosa* (PAO1), *E. coli* O157:H7 (NCIM 5649), *Serratia marcescens* (ATCC 13880) and *Listeria monocytogenes* (ATCC 19114) were used to study the effect of azorubine on virulence functions and biofilm.

2.3. Determination of minimum inhibitory concentration (MIC)

The MIC of azorubine against food-associated bacteria was evaluated, employing TTC in a 96 well Microtitre plate (Patel et al., 2015; Qais et al., 2018). Pathogens were grown in the presence of different concentrations (16–0.125 mg/ml) of azorubine. Post incubation 10 μl of TTC was added to each well and observed for change in color after 20 min. The lowest concentration at which development of pink color was not observed was termed as the MIC.

2.4. Violacein quantification

Violacein was extracted and quantified by the method described previously (Husain et al., 2016). Briefly, azorubine treated and untreated *C. violaceum* 12472 were grown overnight in Luria Bertani (LB) medium. Incubated bacteria (1 ml) was centrifuged to precipitate the violacein. Resultant pellet was suspended in DMSO (1 ml) and vortexed to dissolve the pellet. The solution was centrifuged once again, and absorbance of resultant supernatant was read at 585 nm to quantify the violacein produced.

2.5. Growth curve analysis

The effect of azorubine on the growth of *C. violaceum* 12472 was determined in terms of optical density measured at 600 nm (Husain and Ahmad, 2013).

2.6. Effect on virulence factors produced by P. aeruginosa PAO1

Production of virulence factors (elastase, protease, pyocyanin, and alginate) in treated and untreated cultures of PAO1 was determined using standard protocols described previously (Al-Shabib et al., 2019).

2.7. Extraction and quantification of exopolysaccharides (EPS)

Test pathogens were grown in the absence and presence of respective 0.5 × MIC of azorubine. Cells were harvested by centrifugation, and extraction was done using chilled ethanol (100%) at 4 °C. Quantification was done by estimating sugars (Al-Shabib et al., 2016).

2.8. Swarming motility

Swarming motility of the test pathogens was determined by spotting 5 μl overnight grown culture on LB plates (0.5% agar) amended with 0.5 × MIC of azorubine. Plates without azorubine were taken as untreated control. All plates were incubated for 24 h and the diameter of the swarm was measured.

2.9. Biofilm inhibition

Biofilm inhibition assay was performed by staining with crystal violet (CV) in a 96 well microtitre plate (MTP) as described earlier (Husain et al., 2017). Test pathogens were inoculated into the wells containing 150 μl Tryptic soy broth (TSB). Respective sub-MICs of azorubine were added to each well and incubated for 24 h. Wells containing bacteria and broth were taken as the control group. Post incubation, wells were washed thrice with PBS and dried at room temperature. Subsequently, biofilm in each well was stained with crystal violet (0.1% w/v) for 15 min. Excess stain was washed away. Absorbance was read at 585 nm.

2.10. Light microscopy of biofilm

Overnight grown cultures of all test pathogens were seeded in 12 well plates containing TSB and sterile glass coverslips in absence and presence of 0.5 × MIC of azorubine. Glass coverslips from plates incubated for 24 h under static conditions were rinsed with sterile PBS and stained with 0.1% CV. Air dried, stained coverslips were visualized under a light microscope.

2.11. Visualization of biofilm under scanning electron microscope (SEM) and confocal laser scanning microscope (CLSM)

Biofilm on the coverslip was grown as mentioned above and rinsed with PBS to remove unbound planktonic cells. Washed coverslips were fixed with 2.5% glutaraldehyde and then dehydrated by a gradient of ethanol for 10 min. The air-dried slides were gold coated, and SEM images were obtained using JEOL-JSM 6510 LV, Japan.

For CLSM biofilm were grown as described above, followed by staining with 0.1% acridine orange for 20 min in the dark. CLSM micrographs were recorded using ZEISS LSM780, Germany.

2.12. Mature biofilm disruption assay

Biofilm was allowed to grow for 24 h at 37 °C in 96-well microtitre plate. Planktonic cells that did not adhere were washed away, and fresh TSB was added to each well. Azorubine (0.5 × MIC) was added to each well and incubated overnight. Following incubation, cells were washed thrice with PBS and stained with 0.1% CV solution. Excess stain was removed by washing, and optical density was read at 585 nm.

2.13. ROS generation

ROS generation by treated and untreated bacterial cells were determined using a fluorescent probe 2,7-dichlorofluorescein diacetate (DCFH-DA) as described previously (Qayyum et al., 2017). Bacterial cells growing in the log phase were harvested and mixed with DCFH-DA in the ratio of 1:2000. This mixture was left for shaking at 100 rpm for 30 min. Following incubation, cells were pelleted out and washed with PBS to remove extracellular DCFH-DA. Washed cells were exposed to sub-MICs of azorubine. Fluorescence intensity of the cell suspension was measured at the excitation wavelength of 488 nm and emission wavelength of 535 nm using spectrofluorometer (RFPC5301, Shimadzu, Japan)

2.14. Molecular docking and molecular dynamics simulation

The interaction of azorubine with various proteins involved in quorum sensing such as LasR, Vfr, PqsA and QscR has been evaluated by performing molecular docking and molecular dynamics simulation using different modules of Schrodinger suite in Maestro (Schrödinger, LLC, NY, USA) as described previously (Alajmi et al., 2018a, 2018b; Rehman et al., 2019). Briefly, the structures of ligand (azorubine) was drawn in 2D sketcher and prepared for docking using LigPrep (Schrödinger, LLC, NY, USA). All the possible conformations of ligand were generated at pH 7.0 ± 2.0 using Epik (Schrödinger, LLC, NY, USA) and energy minimized using OPLS3e forcefield. The three-dimensional coordinates of proteins namely LasR (Pdb Id: 2UV0), Vfr (Pdb Id: 2OZ6), PqsA (Pdb Id: 5OE3) and QscR (Pdb Id: 3SZT) were optimized for docking using Glide (Schrödinger, LLC, NY, USA) by removing non-essential water molecules, adding hydrogen atoms, generating any missing side chains and loops using Prime (Schrödinger, LLC, NY, USA) and removing any other heterogeneous molecule except bound ligand, if any. The most probable binding sites on the respective proteins were determined using SiteMap (Schrödinger, LLC, NY, USA). It is significant to note that Vfr has two binding sites (Site 1 and Site 2) on its surface. Grids maps were generated by selecting the centroid of the binding sites as the center of the grid box. The size of grid boxes for LasR, Vfr (Site 1 as well as Site 2), PqsA and QscR were 72 × 72 × 72 Å, 64 × 64 × 64 Å, 64 × 64 × 64 Å, and 72 × 72 × 72 Å respectively. Molecular docking was performed with extra-precision (XP) mode in Glide (Schrödinger, LLC, NY, USA) keeping all the parameters at default values. Further, the docking protocol adopted in this study was first validated by re-docking the respective ligands bound in the X-ray structures of LasR, Vfr, PqsA, and QscR as described earlier (Al-Yousef et al., 2017).

Molecular dynamics simulation was performed using Desmond (Schrödinger, LLC, NY, USA) for 30 ns using NTP ensemble at 300 K temperature and 1 atmospheric bar pressure. An orthorhombic simulation box was generated in the system builder in such a way as the boundaries of the box were at least 10 Å away from the protein. TIP3P explicit solvent model was employed to solvate the simulation box, and proper counterions were added to neutralize the system. Further, 150 mM NaCl was added to the simulation box to mimic the physiological conditions. Before the start of the simulation, the whole system was energy-minimized using OPLS3e forcefield till it converges to 1 kcal/mol/Å. The docking affinity was calculated from the docking energy using the following relation as described earlier (Rehman et al., 2014).

$$\Delta G = -RTlnK_b$$

where R and T are the gas constant (1.987 cal/mol/K) and temperature (298 K) respectively.

3. Results and discussion

In the present study, we first determined the minimum inhibitory concentration (MIC) of azorubine against test pathogens. MIC values were found to be 4 mg/ml against *C. violaceum*, *L. monocytogenes,* and *S. marcescens* while MIC of 8 mg/ml was recorded against *E. coli* and *P. aeruginosa*, respectively. Sub-inhibitory concentrations, i.e. sub-MICs, were used in all assays.

3.1. Effect of azorubine on violacein production

In recent years, disruption of cell-cell signaling (QS) has been explored as an alternative antimicrobial strategy to combat microbial contamination of food and food surfaces. In this regard, *Chromobacterium violaceum* 12472 (CV12472) is the most studied model system to screen QS inhibitors (QSIs) as the production of purple colored violacein pigment is regulated by acyl-homoserine lactone (AHL) dependent QS (McLean et al., 2004). Fig. 1a evidences concentration dependent decrease in the production of violacein by CV12472 in the presence of 0.25–2 mg/ml azorubine. Significant reduction of 28, 41, and 56% over untreated control were recorded

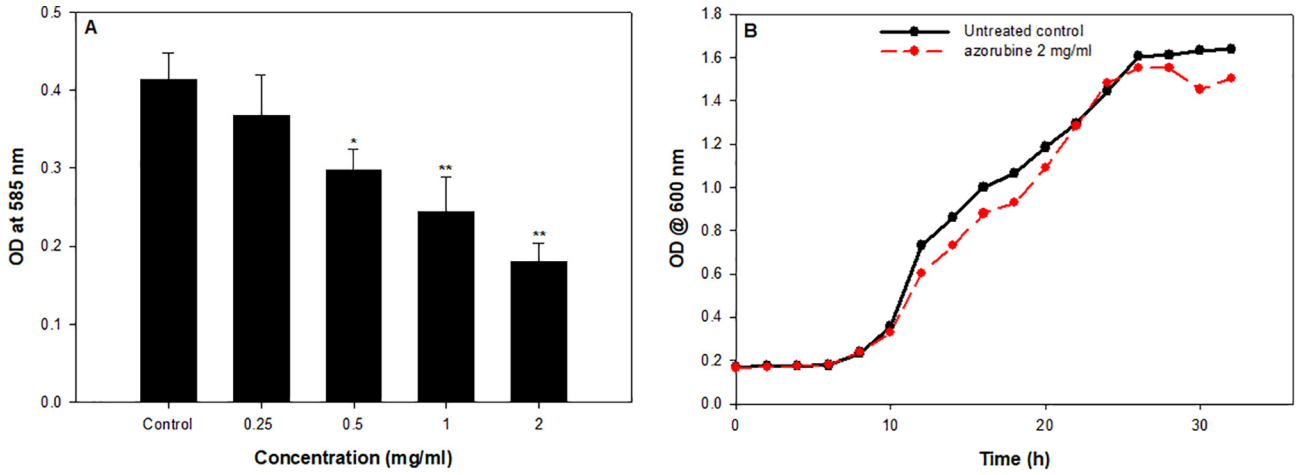

Fig. 1. A. Quantitative determination of violacein inhibition in *C. violaceum* 12472 by sub-MICs of azorubine. Data are represented as mean value of triplicate reading and bars show the SD. * $p \leq 0.05$, ** $p \leq 0.005$ as compared to untreated control. B. Growth curve of *C. violaceum* 12472 in absence and presence of 0.5 × MIC of azorubine.

at 0.5, 1, and 2 mg/ml concentration, respectively. Moreover, growth kinetics studies showed that the viability of the bacteria was not affected significantly after treatment with 2 mg/ml of azorubine (Fig. 1b). Thus, it is envisaged that the reduced production of violacein is due to disruption of (Acyl-homoserine lactone) AHL dependent QS rather than decreased cell population density.

3.2. Effect of azorubine on P. aeruginosa virulence factors

P. aeruginosa has a very complex QS network that regulates the production of an array of virulence functions. These secreted virulence determinants govern the pathogenicity in *P. aeruginosa* by facilitating its survival, colonization, and invasion leading to chronic, persistent, and recurring infections (Chatterjee et al., 2016). In the current investigation, the effect of azorubine was determined against QS-regulated virulence factors produced by *P. aeruginosa* PAO1. Elastase and protease play a vital role in the invasion and colonization of the host by damaging the epithelial barriers (Sarabhai et al., 2013). Significant decrease in the elastase production of PAO1 was recorded upon exposure to sub-inhibitory concentration of the food colorant. Azorubine demonstrated 6–44% reduction in elastolytic activity at concentrations ranging from 0.5 to 4 mg/ml (Fig. 2). Further, the protease activity of PAO1 was lowered substantially upon treatment with the test agent. Inhibition of 15–57% was observed in comparison to the untreated control (Fig. 2). Consistent with present data, Husain et al., (2016) demonstrated significantly impaired elastolytic and proteolytic activity in PAO1 upon treatment with sub-MICs of antibiotic ceftazidime. Pyocyanin is another vital cog in the armory of *P. aeruginosa*, it is a phenazine compound, toxic and plays a crucial role during the infection process by causing cytotoxicity (Fothergill et al., 2014). Therefore, the effect of sub-MICs of azorubine on the ability of the bacteria to produce pyocyanin was examined. Production of pyocyanin pigment decreased with increasing concentration, demonstrating 49% inhibition upon treatment with 4 mg/ml concentration of azorubine as compared to the untreated control (Fig. 2). As observed in the present study, notable reduction in pyocyanin production was recorded with N-decanoyl cyclopentylamide (36%) and doxycycline (69%) (Husain and Ahmad, 2013; Ishida et al., 2007). Alginate is one of the chief component of the exopolysaccharides (EPS) secreted by *P. aeruginosa* PAO1 during biofilm formation. It helps in maintaining biofilm architecture and prevents the entry of antimicrobials making bacteria residing in biofilm mode more resistant (Gopu et al., 2015).

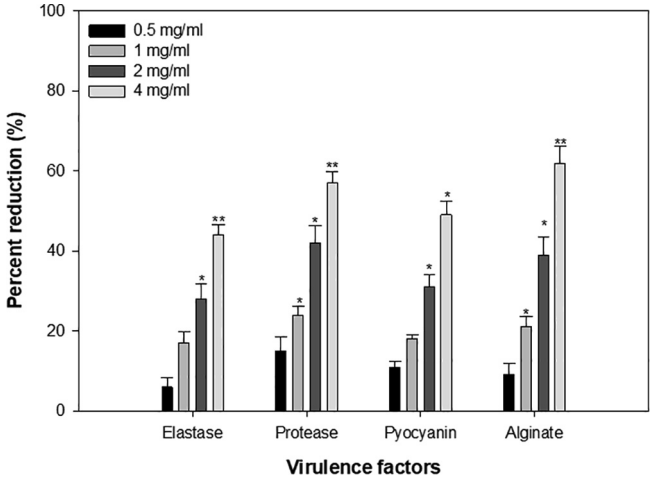

Fig. 2. Effect of azorubine on the production of virulence factors in *P. aeruginosa* PAO1 at 0.5, 1, 2, 4 mg/ml. Data are represented as mean value of triplicate reading and bars show the SD. * $p \leq 0.05$, ** $p \leq 0.005$ as compared to untreated control.

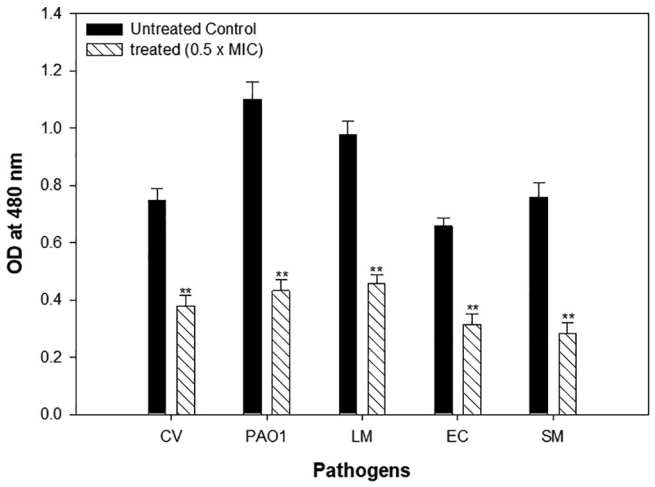

Fig. 3. Effect of sub-MICs of azorubine on the production of EPS in test pathogens. Data are represented as mean value of triplicate reading and bars show the SD. ** $p \leq 0.005$ as compared to untreated control. *Chromobacterium violaceum* ATCC 12472 (CV); *Pseudomonas aeruginosa* PAO1 (PAO1), *E. coli* O157:H7 NCIM 5649 (EC), *Serratia marcescens* ATCC 13880 (SM) and *Listeria monocytogenes* ATCC 19114 (LM).

Efficacy of azorubine in attenuating alginate production at sub-MICs was studied, and concentration dependent reduction was recorded. Highest reduction of 62% was recorded at 4 mg/ml while at 0.5 mg/ml concentration, 9% decrease was observed (Fig. 2). Findings of the present study substantiated with the report showing inhibition of alginate production on treatment with Sodium houttuyfonate and food color curcumin (Packiavathy et al., 2014; Wu et al., 2015).

3.3. Effect on EPS production and swarming motility

EPS production is vital for the formation and maintenance of biofilm architecture as it provides strength and structure to the matrix. Moreover, it is responsible for conferring resistance to the biofilm by protecting the cells from the action of antimicrobial drugs (Mah and O'Toole, 2001). Significant decrease in the EPS production in test pathogens was recorded when grown in the presence of 0.5 × MIC of azorubine. As evidenced from the Fig. 3, production of EPS was impaired by 49, 61, 53, 53 and 63% in *C. violaceum*, PAO1, *L. monocytogenes*, *E. coli*, and *S. marcescens*, respectively over untreated control (Fig. 3). The results obtained corroborate well with findings on copper (I) complexes with β-carboline wherein comparable reduction in EPS of food-borne pathogens was recorded at sub-MICs (Al-Shabib et al., 2019).

Development of biofilm starts with the adherence of the bacterial cells to the substratum. This adherence of bacterial cells and

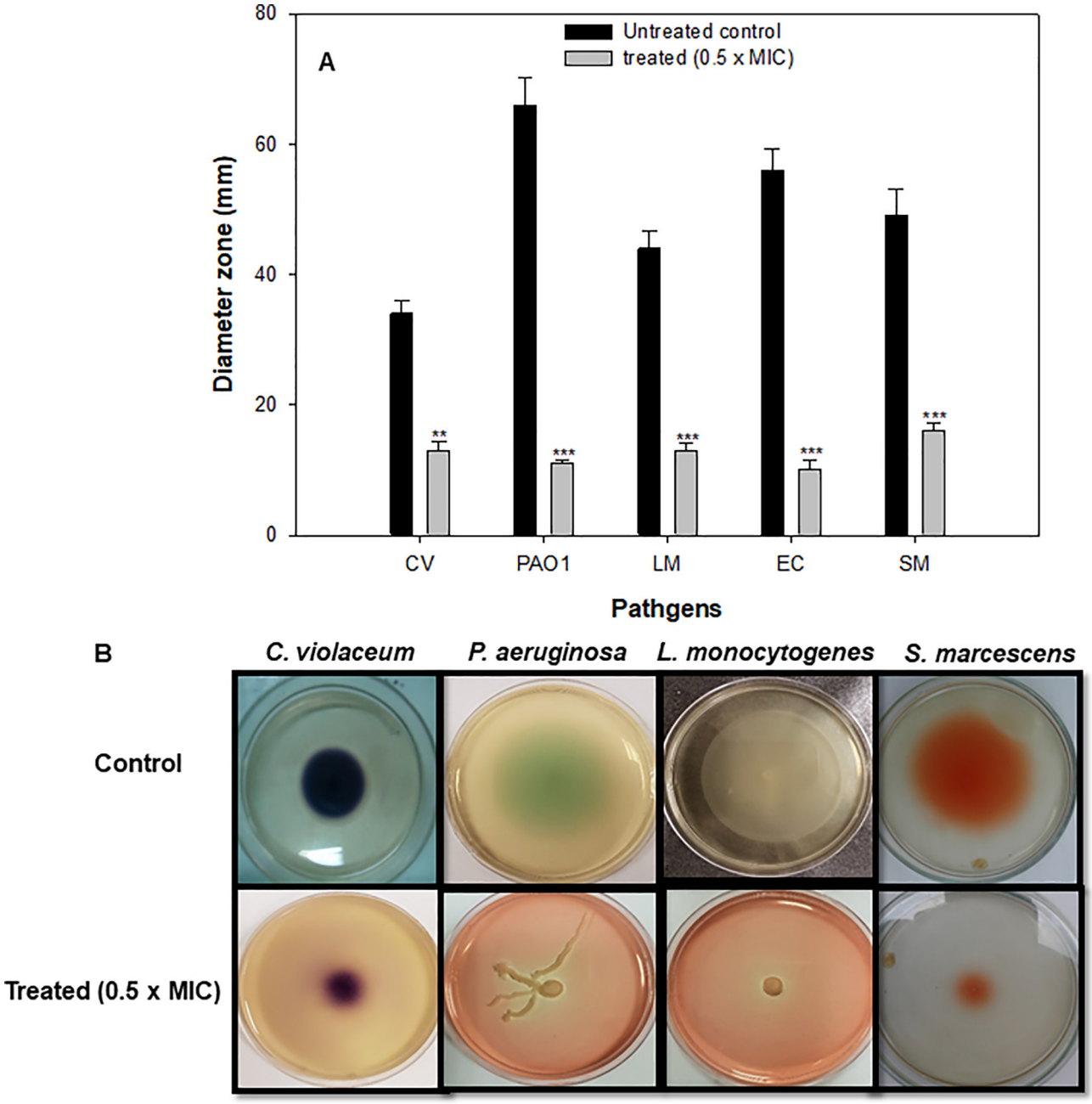

Fig. 4. A. Reduction in swarming motility of test pathogen after treatment with 0.5 × MIC of azorubine. Data are represented as mean value of triplicate readings and bars show the SD. ** $p \leq 0.005$, *** $p \leq 0.001$ as compared to untreated control. B. Plates demonstrating decrease in the diameter of swarm of the test pathogens of untreated control; azorubine (0.5 × MIC) treated cultures. *Chromobacterium violaceum* ATCC 12472 (CV); *Pseudomonas aeruginosa* PAO1 (PAO1), *E. coli* O157:H7 NCIM 5649 (EC), *Serratia marcescens* ATCC 13880 (SM) and *Listeria monocytogenes* ATCC 19114 (LM).

colonization for biofilm formation are facilitated by the swarming motility (Al-Shabib et al., 2018a). Therefore, it is considered as a vital function in the establishment of biofilm, and any interference with the motility is deemed detrimental for the formation of resistant biofilm. In our study, migration of the bacterial pathogens was arrested significantly over untreated control at tested concentrations of the colorant (Fig. 4a). The diameter of the swarm was reduced by 61, 83, 70, 82 and 67% in *C. violaceum*, PAO1, *L. monocytogenes*, *E. coli,* and *S. marcescens*, respectively at 0.5 × MIC as depicted in Fig. 4b. Our results find support from the observations on curcumin wherein it inhibited the swarming motility of *Escherichia coli*, *Pseudomonas aeruginosa* PAO1, *Proteus mirabilis,* and *Serratia marcescens* significantly at tested sub-MICs (Packiavathy et al., 2014).

3.4. Biofilm inhibition activity

Attachment of bacteria leading to the formation of biofilm is undesirable and harmful to food systems. Biofilm provides physical and mechanical resistance to the microbes and protects them against chemicals, disinfectants, and antimicrobials used in the food industry. Moreover, the formation of biofilm in the food industry risks human health as food-borne diseases associated with biofilm are caused due to the intoxication or infection (Galié et al., 2018). In this context, targeting biofilm could be of prime importance in limiting food-borne diseases. In the present investigation, at 0.5 × MIC, significant reduction in biofilm formation was recorded in all test pathogens. The percentage inhibition was observed to be 50, 65, 60, 45 and 57% in *C. violaceum*, PAO1, *L. monocytogenes*, *E. coli,* and *S. marcescens*, respectively as compared to untreated control (Fig. 5). Azorubine depicted broad-spectrum biofilm inhibitory potency against food-associated bacteria. The findings are in agreement with the report on biofilm inhibition by ceftazidime (Husain et al., 2016). Al-Shabib et al. (2019) demonstrated three copper (I) complexes as promising inhibitors of biofilm against food-associated bacteria.

Microscopic analysis of biofilm inhibition was done using light microscopy, CLSM, and SEM (Fig. 5). Microscopic images of the treated samples showed disturbed architecture, cells were found to be scattered, and cell clusters were also reduced due to poor aggregation and adherence while untreated biofilm showed highly dense aggregation of bacterial cells. Biofilm microscopy analysis is in agreement with the quantitative results observed in the previous sections.

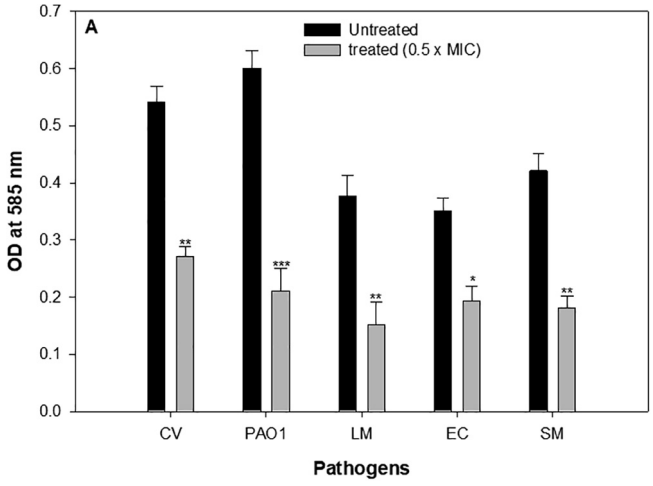

Fig. 5. A. Inhibitory action of azorubine on the biofilm formation in tests bacteria using crystal violet assay. Data are represented as mean value of triplicate readings and bars show the SD. * $p \leq 0.05$, ** $p \leq 0.005$, *** $p \leq 0.001$ as compared to untreated control. B. Light microscopy, scanning electron microscopy (SEM) and confocal laser scanning microscopy (CLSM) images of untreated control and azorubine treated biofilm inhibition.

3.5. Inhibition of mature biofilm

Bacteria residing in biofilm mode are 1000 times more resistant to antimicrobials and chemical disinfectants, and thus, their eradication is also challenging (Jw et al., 1999). Azorubine was tested for its ability to eliminate pre-formed biofilm. The assay revealed that 0.5 × MIC, 47% of the biofilm was eradicated in *C. violaceum* (Fig. 6). For *P. aeruginosa* and *L. monocytogenes*, azorubine reduced the pre-formed biofilm by 54 and 49%, respectively.

Similarly, 24 h mature biofilms formed by *E. coli* and *S. marcescens* were diminished by 50 and 52%, respectively, in comparison to the untreated biofilms. The data presented in Fig. 6 clearly shows the effectiveness of azorubine in degrading pre-formed (mature) biofilm in both gram-negative and gram-positive food associated pathogens. Based on the findings on the reduction of EPS and alginate production, it is envisaged that azorubine penetrates the biofilm and eliminates preformed biofilm in all test pathogens significantly.

3.6. ROS generation

The relative amount of ROS generated by azorubine was determined using the fluorescent dye DCFH-DA. Fig. 7 shows the ROS generation in the treated and untreated pathogens. Exposure of pathogenic bacteria to 0.5 × MIC of azorubine resulted in significant increase in ROS production. In the presence of tested sub-MIC of the colorant, C. violaceum exhibited 59% enhancement in ROS levels. Similarly, the amount of ROS in PAO1, *L. monocytogenes*, *E. coli,* and *S. marcescens* was boosted by 69, 28, 72 and 53% in comparison to untreated cells. ROS causes loss of viability in bacterial cells by damaging DNA, proteins, and lipids and it is also responsible for the altered expression of virulence factors in the pathogens (Qais et al., 2018). Thus, it is envisaged that ROS generation in treated cells results in cell death leading to reduced biofilm formation (Al-Shabib et al., 2018b; Qayyum et al., 2017). Our observations suggest that in addition to the disruption of QS circuit, ROS generation in the test pathogens may also be responsible for the inhibition of biofilm by sub-MICs of azorubine.

3.7. Molecular docking and molecular dynamics simulation

The binding of azorubine with virulent proteins (LasR, Vfr, PqsA, and QscR) was studied by performing molecular docking along with molecular dynamics simulation, and the results are presented in Table 1. We found a weak interaction of azorubine with LasR and Vfr (site I) since their docking energies were estimated to be −2.592, and −3.423 kcal/mol respectively. Conversely, a moderate interaction with docking energy of −4.345 kcal/mol, and strong interaction with docking energy of −6.704 kcal/mol have been observed for azorubine towards Vfr site II and PqsR respectively. Moreover, we found that azorubine did not show any binding with QscR (Table 1).

In depth analysis of the X-ray crystal structure of Vfr has shown that site II is the binding site for cAMP (Cordes et al., 2011). The Vfr-cAMP complex was stabilized principally by hydrophobic (p-alkyl interaction) interactions with Ile51, Ile63, Ala89, and Arg128 of Vfr. In this study, the molecular docking of azorubine at the binding site II of Vfr has shown that azorubine formed one hydrogen bond with Gly73, and ten hydrophobic interactions with Ile51, Ile53, Ile63, Leu66, Phe72, Leu75, Ala89, Val91, Met125 and Leu129 (Table 1 and Fig. 8A, B). Further, other residues such as

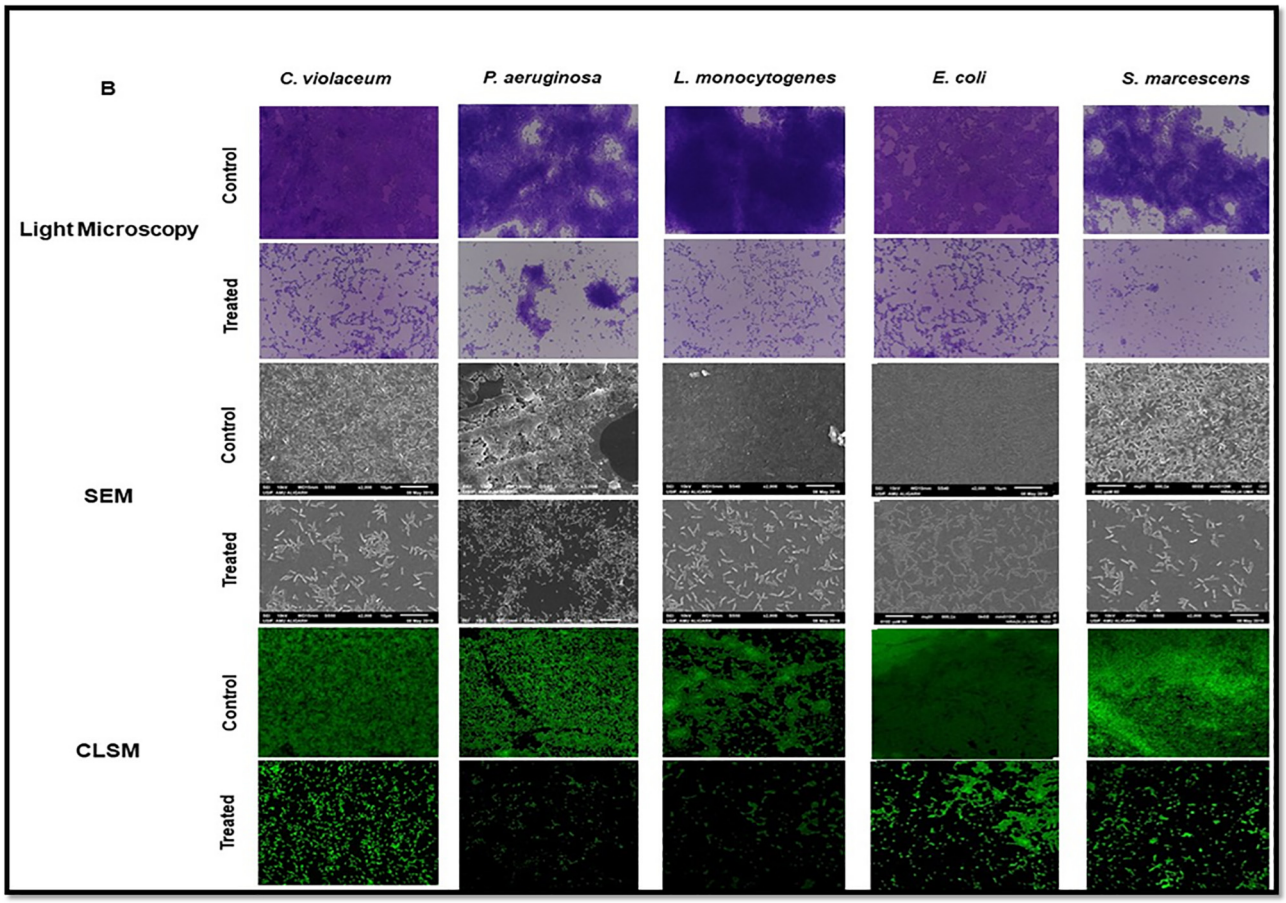

Fig. 5 (*continued*)

Ser88, Glu74, Arg128, and Thr132 also play crucial roles in stabilizing azorubine-Vfr complex at site II. It is worth noticing that the residues Ile51, Ile63, Ala89, and Arg128 of Vfr were commonly occupied by cAMP and azorubine. Moreover, the docking energy and docking affinity of azorubine towards Vfr were estimated to be −4.345 kcal/mol and 1.54×10^3 M^{-1}, respectively. Previously, it is reported that quercetin 4Ó-*O*- β-D glucopyranoside (QGP) inhibits quorum sensing mediated biofilm formation in *Chromobacterium violaceum* CV12472 and *Pseudomonas aeruginosa* PAO1 by binding at site II of Vfr (Al-Yousef et al., 2017).

The X-ray crystal structure of N-terminal domain of PqsA in complex with anthraniloyl-AMP revealed that it formed seven hydrogen bonds (three Asp282, two with Thr304, and one with Asp299, and Gly300) and six hydrophobic interactions (Phe209,

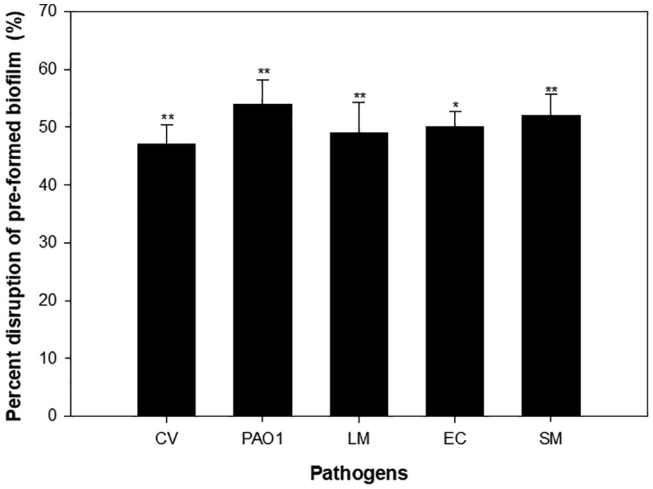

Fig. 6. Effect of sub-MICs of azorubine on pre-formed (mature) biofilm. Data are represented as mean value of triplicate readings and bars show the SD. * $p \leq 0.05$, ** $p \leq 0.005$, as compared to untreated control.

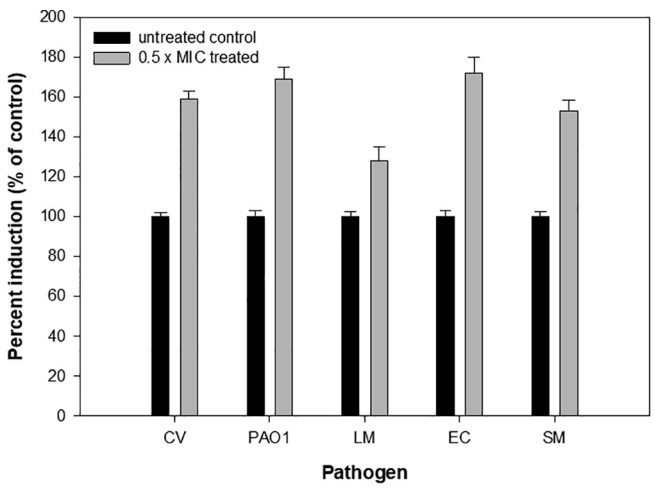

Fig. 7. Azorubine induced ROS generation in treated and untreated *Chromobacterium violaceum*, *Pseudomonas aeruginosa*, *E. coli* O157:H7, *Serratia marcescens* and *Listeria monocytogenes*.

Table 1
Interaction of Azorubine with different proteins involved in quorum sensing.

	LasR	Vfr		PqsA	QscR
		Site 1	Site 2		
Hydrogen bonds	Cys79	Glu60, Arg185*	Gly73	Thr304*	NB
Hydrophobic interactions	Leu36, Leu39, Leu40, Tyr47, Ala50, Phe51, Ile52, Trp60, Val76, Trp88 Tyr93, Phe101, Ala105, Leu110, Leu125, Ala127	Met61, Leu139, Cys183	Ile51, Ile53, Ile63, Leu66, Phe72, Leu75, Ala89, Val91, Met125, Leu129	Phe209, Tyr211, Ala278, Ile301, Ala303, Val309, Phe310, Tyr378	NB
Salt bridges	–	Arg59, Arg185	–	Arg372, Arg397	NB
Pi-Pi stacking	Tyr56, Tyr64				NB
Other residues	Gly38, Arg61, Asp73, Thr75, Thr80, Thr115, Gly126, Ser129	Gly58, Gln175, Gly178, Arg179, Gly182, Ser184	Ser88, Glu74, Arg128, Thr132	Thr164, Gly210, Gly279, Gly302, Glu305, Hie308, Thr380, Gly381, Asp382	NB
Docking energy (kcal/mol)	−2.592	−3.423	−4.345	−6.704	NB
Docking affinity (M^{-1})	79.63	324.04	1.54×10^3	8.26×10^5	NB

NB: No binding.
* Indicated that the residue formed two hydrogen bonds.

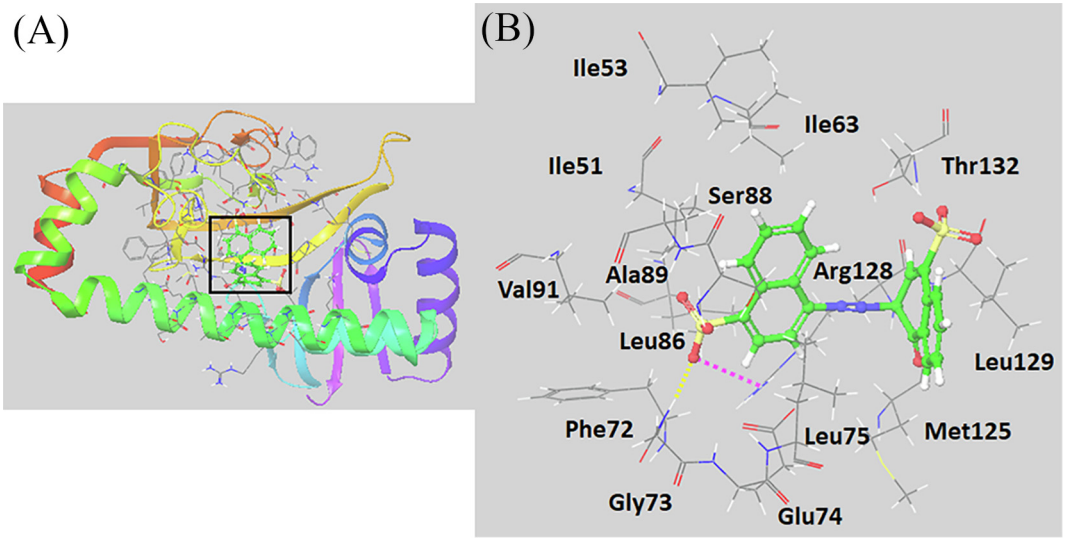

Fig. 8. (A) Molecular docking of azorubine at the active site of Vfr, and (B) molecular interaction between azorubine and Vfr. Hydrogen bonds are shown in the yellow dash line while salt bridges are shown in the pink dashed lines.

Tyr211, Ala278, His308, and Val309) (Witzgall et al., 2017) Our molecular docking analysis revealed that azorubine interacted with the active site residues of PqsA by forming one hydrogen bond with Thr304, and eight hydrophobic interactions with Phe209, Tyr211, Ala278, Ile301, Ala303, Val309, Phe310, and Tyr378 and two salt-bridges with Arg372 and Arg397 (Table 1 and Fig. 9A, B). Moreover, the PqsA-azorubine complex was additionally stabilized by other amino acid residues such as Thr164, Gly210, Gly279, Gly302, Glu305, Hie308, Thr380, Gly381, and Asp382. The overall docking energy and the corresponding docking affinity of azorubine towards PqsA were estimated to be −6.704 kcal/mol and 8.26×10^6 M^{-1} respectively.

The stability of azorubine-PqsA complex was evaluated by performing molecular dynamics simulation for 30 ns at 300 K. The analysis of RMSD indicates if the simulation has equilibrated or not and thus gives the information about the structural conformation of a protein for the entire simulation period. For an adequately equilibrated and stable system, the fluctuations towards the end of the simulation should be within 1–3 Å for a globular protein. Changes are higher than that, however, suggest that the protein is undergoing significant conformational change during the simulation. In this work, the RMSD values of PqsA remained constant around ~1.25–1.35 Å in the absence as well as the presence of azorubine, implying a stable conformation of the protein (Fig. 10A). The analysis of RMSD values indicates that azorubine binds at the active site of PqsA and the azorubine-PqsA complex remains stable. The radius of gyration (rGyr) of azorubine also remains constant throughout the simulation time, indicating that azorubine does not undergo a major conformational change (Fig. 10B). The formation of a stable azorubine-PqsA complex was also suggested by observing the change in various surface areas such as molecular surface area (MolSA), polar surface area (PSA), and solvent accessible surface area (SASA) of the azorubine-PqsA complex as a function of simulation time. We observed that MolSA, PSA and SASA remained persistent within the prescribed limits, thus confirming a stable complex between azorubine and PqsA (Fig. 9B). The local conformational changes along PqsA chain were probed by analyzing the root mean square fluctuation (RMSF) with respect to simulation time (Fig. 10D). The areas of PqsA which fluctuate the most (indicated in blue) during simulation coincide with

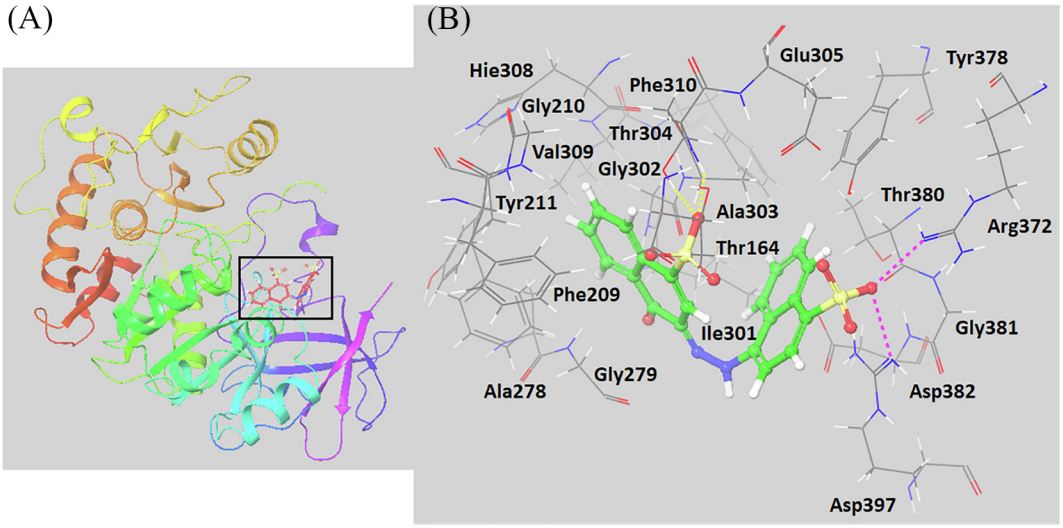

Fig. 9. (A) Molecular docking of azorubine at the active site of PqsA, and (B) molecular interaction between azorubine and PqsA. Hydrogen bonds are shown in the yellow dash line while salt bridges are shown in the pink dashed lines.

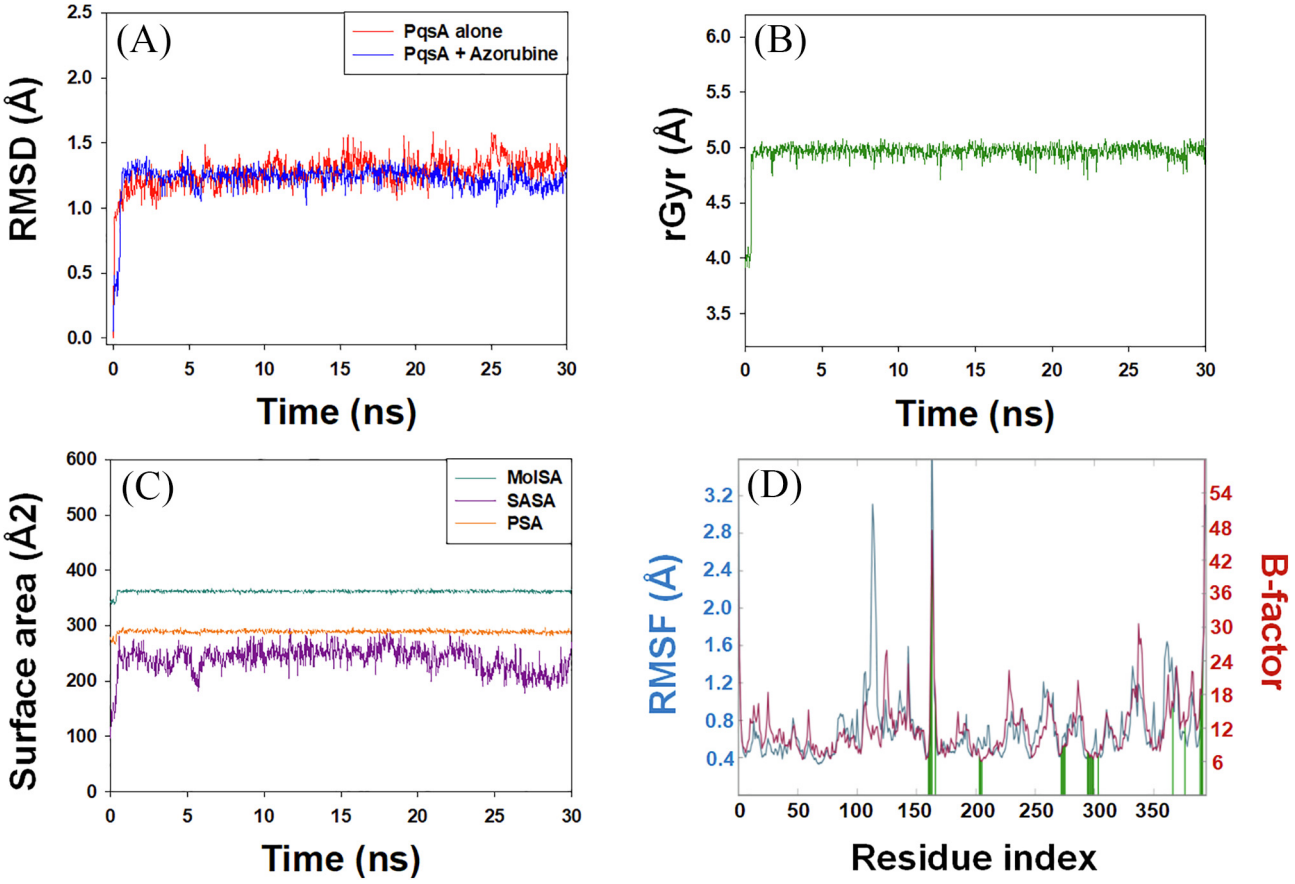

Fig. 10. Molecular dynamics simulation of azorubine with PqsA. (A) root mean square deviations (RMSDs) of PqsA in the absence and presence of azorubine, (B) radius of gyrastion (rGyr) of azorubine as a function of simulation time, (C) variations in molecular surface area (MolSA), solvent accessible surface area (SASA) and polar surface area (PSA) of azorubine as a function of simulation time, and (D) root mean square fluctuations (RMSFs) in PqsA in the presence of azorubine as a function of simulation time.

the X-ray determined B-factor (indicated in dark red). Furthermore, the vertical green lines on the X-axis show the interaction between PqsA and azorubine.

It is clear from the molecular docking and molecular dynamics simulation studies that azorubine binds strongly to PqsA as compared to other virulent proteins (LasR, Vfr and QscR). Thus, the pos-

sible quorum sensing inhibitory activity of azorubine can be attributed to the inhibition of PqsA controlled pathway. PqsA is the first enzyme in an autoinducer-regulated *pqs* pathway of quorum sensing.

4. Conclusion

In the present investigation, food colorant 'azorubine' was found to possess QS inhibitory properties. *In vitro* assays showed broad-spectrum interference of quorum sensing regulated virulence by sub-inhibitory concentrations of azorubine against food-associated bacteria. Further, reduced biofilm formation and obliteration of pre-formed biofilms were also recorded in all the test pathogens. This biofilm inhibitory action of azorubine can be attributed to the interference with the QS circuit of the test pathogens. Additionally, the generation of ROS molecules by the interaction of the colorant and bacterial cells could also be responsible for the obliteration of biofilm in both Gram-positive and Gram-negative bacteria. Further, molecular docking and simulation studies with QS virulent protein revealed that the plausible quorum sensing inhibitory activity of azorubine can be attributed to the inhibition of PqsA controlled pathway as it shows strong binding affinity with PqsA. Therefore, it is envisaged that in addition to the enhancement of appeal of the food items, azorubine, can also be exploited by the food industry as an anti-QS and anti-biofilm agent to prevent food spoilage and reduce economic losses.

Declaration of Competing Interest

The authors declare that they have no known competing financial interests or personal relationships that could have appeared to influence the work reported in this paper.

Acknowledgment

The authors extend their appreciation to Deanship of Scientific Research at King Saud University for funding this work through Research Group No. RGP-1439-014.

References

Al-Shabib, N.A., Husain, F.M., Ahmad, N., Qais, F.A., Khan, A., Khan, A., et al., 2018a. Facile synthesis of tin oxide hollow nanoflowers interfering with quorum sensing-regulated functions and bacterial biofilms. J. Nanomater. 2018, 1–11. https://doi.org/10.1155/2018/6845026.

Al-Shabib, N.A., Husain, F.M., Ahmed, F., Khan, R.A., Ahmad, I., Alsharaeh, E., et al., 2016. Biogenic synthesis of Zinc oxide nanostructures from Nigella sativa seed: prospective role as food packaging material inhibiting broad-spectrum quorum sensing and biofilm. Sci. Rep. 6. https://doi.org/10.1038/srep36761.

Al-Shabib, N.A., Husain, F.M., Ahmed, F., Khan, R.A., Khan, M.S., Ansari, F.A., et al., 2018b. Low temperature synthesis of superparamagnetic iron oxide (Fe_3O_4) nanoparticles and their ROS mediated inhibition of biofilm formed by food-associated bacteria. Front. Microbiol. 9, 2567. https://doi.org/10.3389/fmicb.2018.02567.

Al-Shabib, N.A., Husain, F.M., Khan, R.A., Khan, M.S., Alam, M.Z., Ansari, F.A., et al., 2019. Interference of phosphane copper (I) complexes of β-carboline with quorum sensing regulated virulence functions and biofilm in foodborne pathogenic bacteria: a first report. Saudi J. Biol. Sci. 26, 308–316. https://doi.org/10.1016/j.sjbs.2018.04.013.

Al-Yousef, H.M., Ahmed, A.F., Al-Shabib, N.A., Laeeq, S., Khan, R.A., Rehman, M.T., et al., 2017. Onion peel ethylacetate fraction and its derived constituent quercetin 40-O-β-D glucopyranoside attenuates quorum sensing regulated virulence and biofilm formation. Front. Microbiol. 8. https://doi.org/10.3389/fmicb.2017.01675.

Alajmi, M.F., Alam, P., Rehman, M.T., Husain, F.M., Khan, A.A., Siddiqui, N.A., et al., 2018a. Interspecies anticancer and antimicrobial activities of genus solanum and estimation of rutin by validated UPLC-PDA Method. Evid.-based Compl. Altern. Med. 2018. https://doi.org/10.1155/2018/6040815.

AlAjmi, M.F., Rehman, M.T., Hussain, A., Rather, G.M., 2018b. Pharmacoinformatics approach for the identification of Polo-like kinase-1 inhibitors from natural sources as anti-cancer agents. Int. J. Biol. Macromol. 116, 173–181. https://doi.org/10.1016/j.ijbiomac.2018.05.023.

Amin, K.A., Abdel Hameid, H., Abd Elsttar, A.H., 2010. Effect of food azo dyes tartrazine and carmoisine on biochemical parameters related to renal, hepatic function and oxidative stress biomarkers in young male rats. Food Chem. Toxicol. 48, 2994–2999. https://doi.org/10.1016/j.fct.2010.07.039.

Bai, A.J., Rai, V.R., 2011. Bacterial quorum sensing and food industry. Compr. Rev. Food Sci. Food Saf. 10, 183–193. https://doi.org/10.1111/j.1541-4337.2011.00150.x.

Basu, A., Kumar, G.S., 2014. Study on the interaction of the toxic food additive carmoisine with serum albumins: a microcalorimetric investigation. J. Hazard. Mater. 273, 200–206. https://doi.org/10.1016/j.jhazmat.2014.03.049.

Basu, A., Suresh Kumar, G., 2014. Minor groove binding of the food colorant carmoisine to DNA: spectroscopic and calorimetric characterization studies. J. Agric. Food Chem. 62, 317–326. https://doi.org/10.1021/jf404960n.

Basu, A., Suresh Kumar, G., 2015. Binding of carmoisine, a food colorant, with hemoglobin: spectroscopic and calorimetric studies. Food Res. Int. 72, 54–61. https://doi.org/10.1016/j.foodres.2015.03.015.

Chatterjee, M., Anju, C.P., Biswas, L., Anil Kumar, V., Gopi Mohan, C., Biswas, R., 2016. Antibiotic resistance in *Pseudomonas aeruginosa* and alternative therapeutic options. Int. J. Med. Microbiol. 306, 48–58. https://doi.org/10.1016/j.ijmm.2015.11.004.

Cordes, T.J., Worzalla, G.A., Ginster, A.M., Forest, K.T., 2011. Crystal structure of the *Pseudomonas aeruginosa* virulence factor regulator. J. Bacteriol. 193, 4069–4074. https://doi.org/10.1128/JB.00666-10.

Fothergill, J.L., James, C.E., Winstanley, C., 2014. Novel therapeutic strategies to counter *Pseudomonas aeruginosa* infections. Exp. Rev. Anti-infect. Ther. 10, 1–28. https://doi.org/10.1586/eri.11.168.

Galié, S., García-Gutiérrez, C., Miguélez, E.M., Villar, C.J., Lombó, F., 2018. Biofilms in the food industry: Health aspects and control methods. Front. Microbiol. 9, 1–18. https://doi.org/10.3389/fmicb.2018.00898.

Gopu, V., Meena, C.K., Shetty, P.H., 2015. Quercetin influences quorum sensing in food borne bacteria: In-vitro and in-silico evidence. PLoS One 10, 1–17. https://doi.org/10.1371/journal.pone.0134684.

Hallagan, J.B., Allen, D.C., Borzelleca, J.F., 1995. The safety and regulatory status of food, drug and cosmetics colour additives exempt from certification. Food Chem. Toxicol. 33, 515–528. https://doi.org/10.1016/0278-6915(95)00010-Y.

Høiby, N., Bjarnsholt, T., Givskov, M., Molin, S., Ciofu, O., 2010. Antibiotic resistance of bacterial biofilms. Int. J. Antimicrob. Age. 35, 322–332. https://doi.org/10.1016/j.ijantimicag.2009.12.011.

Husain, F.M., Ahmad, I., 2013. Doxycycline interferes with quorum sensing-mediated virulence factors and biofilm formation in Gram-negative bacteria. World J. Microbiol. Biotechnol. 29. https://doi.org/10.1007/s11274-013-1252-1.

Husain, F.M., Ahmad, I., Al-Thubiani, A.S., Abulreesh, H.H., AlHazza, I.M., Aqil, F., 2017. Leaf extracts of Mangifera indica L. inhibit quorum sensing - regulated production of virulence factors and biofilm in test bacteria. Front. Microbiol. 8. https://doi.org/10.3389/fmicb.2017.00727.

Husain, F.M., Ahmad, I., Baig, M.H., Khan, M.S., Khan, M.S., Hassan, I., et al., 2016. Broad-spectrum inhibition of AHL-regulated virulence factors and biofilms by sub-inhibitory concentrations of ceftazidime. RSC Adv. 6. https://doi.org/10.1039/c6ra02704k.

Ishida, T., Ikeda, T., Takiguchi, N., Kuroda, A., Ohtake, H., Kato, J., 2007. Inhibition of quorum sensing in *Pseudomonas aeruginosa* by N-acyl cyclopentylamides. Appl. Environ. Microbiol. 73, 3183–3188. https://doi.org/10.1128/AEM.02233-06.

Johnson, L.R., 2008. Microcolony and biofilm formation as a survival strategy for bacteria. J. Theor. Biol. 251, 24–34. https://doi.org/10.1016/j.jtbi.2007.10.039.

Jw, C., Ps, S., Ep, G., 1999. Bacterial biofilms: a common cause of persistent infections. Science (80-.) 284, 1318. https://doi.org/10.1126/science.284.5418.1318.

Khan, A.A., Sutherland, J.B., Khan, M.S., Abdullah, S., 2017. Location of Biofilm and Quorum Sensing Inhibitors Food Preservative, pp. 439–463.

LaSarre, B., Federle, M.J., 2013. Exploiting quorum sensing to confuse bacterial pathogens. Microbiol. Mol. Biol. Rev. 77, 73–111. https://doi.org/10.1128/MMBR.00046-12.

Mah, C. Thien Fah, O'Toole, George A., 2001. Mechanisms of biofilm resistance to antimicrobial agents. Trends Microbiol. 9, 34–39. https://doi.org/10.1016/S0966-842X(00)01913-2.

McLean, R.J.C., Pierson, L.S., Fuqua, C., 2004. A simple screening protocol for the identification of quorum signal antagonists. J. Microbiol. Meth. 58, 351–360. https://doi.org/10.1016/j.mimet.2004.04.016.

Nguyen, D., Amruta, J.D., Francois, L., Elizabeth, B., Oyebode, O., Karlyn, B., et al., 2011. Active starvation responses mediate antibiotic tolerance in biofilms and nutrient-limited bacteria. Science (80-.) 334, 982–986. https://doi.org/10.1126/science.1211037.Active.

Obón, J.M., Castellar, M.R., Cascales, J.A., Fernández-López, J.A., 2005. Assessment of the TEAC method for determining the antioxidant capacity of synthetic red food colorants. Food Res. Int. 38, 843–845. https://doi.org/10.1016/j.foodres.2005.01.010.

Packiavathy, I.A.S.V., Priya, S., Pandian, S.K., Ravi, A.V., 2014. Inhibition of biofilm development of uropathogens by curcumin - an anti-quorum sensing agent from Curcuma longa. Food Chem. 148, 453–460. https://doi.org/10.1016/j.foodchem.2012.08.002.

Parsek, M.R., Greenberg, E.P., 2005. Sociomicrobiology: the connections between quorum sensing and biofilms. Trends Microbiol. 13, 27–33. https://doi.org/10.1016/j.tim.2004.11.007.

Patel J.B., Cockerill R.F., Bradford A.P., Eliopoulos M.G., Hindler A.J., Jenkins G.S., Lewis S.J., Limbago B., Miller A.L., Nicolau P.D., Pwell M., Swenson M.J., Traczewski M.M., Turnidge J.D., W.P.M.Z.L.B., 2015. M07-A10: Methods for Dilution Antimicrobial Susceptibility Tests for Bacteria That Grow Aerobically;

Approved Standard, tenth ed. CLSI (Clinical Lab. Stand. Institute), pp. 35. https://doi.org/10.1007/s00259-009-1334-3.
Qais, F.A., Samreen, Ahmad I., Abul Qais, F., Samreen, Ahmad, I., 2018. Broad-spectrum inhibitory effect of green synthesised silver nanoparticles from Withania somnifera (L.) on microbial growth, biofilm and respiration: a putative mechanistic approach. IET Nanobiotechnol. 12, 325–335. https://doi.org/10.1016/j.actbio.2005.02.008.
Qayyum, S., Oves, M., Khan, A.U., 2017. Obliteration of bacterial growth and biofilm through ROS generation by facilely synthesized green silver nanoparticles. PLoS One 12, 1–18. https://doi.org/10.1371/journal.pone.0181363.
Rehman, M.T., Alajmi, M.F., Hussain, A., Rather, G.M., Khan, M.A., 2019. High-throughput virtual screening, molecular dynamics simulation, and enzyme kinetics identified ZINC84525623 as a potential inhibitor of NDM-1. Int. J. Mol. Sci. 20. https://doi.org/10.3390/ijms20040819.
Rehman, M.T., Shamsi, H., Khan, A.U., 2014. Insight into the binding mechanism of imipenem to human serum albumin by spectroscopic and computational approaches. Mol. Pharm. 11, 1785–1797. https://doi.org/10.1021/mp500116c.
Rutherford, S.T., Bassler, B.L., Delany, I., Rappuoli, R., Seib, K.L., Ben-tekaya, H., et al., 2014. Bacterial quorum sensing: its role in virulence and possibilities for its control, pp. 1–26. https://doi.org/10.1101/cshperspect.a012427.
Sarabhai, S., Sharma, P., Capalash, N., 2013. Ellagic acid derivatives from Terminalia chebula Retz. downregulate the expression of quorum sensing genes to attenuate *Pseudomonas aeruginosa* PAO1 virulence. PLoS One 8, 1–11. https://doi.org/10.1371/journal.pone.0053441.
Skandamis, P.N., Nychas, G.-J.E., 2012. Quorum Sensing in the context of food microbiology. Appl. Environ. Microbiol. 78, 5473–5482. https://doi.org/10.1128/aem.00468-12.
Solano, C., Echeverz, M., Lasa, I., 2014. Biofilm dispersion and quorum sensing. Curr. Opin. Microbiol. 18, 96–104. https://doi.org/10.1016/j.mib.2014.02.008.
Witzgall, F., Ewert, W., Blankenfeldt, W., 2017. Structures of the N-terminal domain of PqsA in complex with anthraniloyl- and 6-fluoroanthraniloyl-AMP: substrate activation in pseudomonas quinolone signal (PQS) biosynthesis. ChemBioChem 18, 2045–2055. https://doi.org/10.1002/cbic.201700374.
Wu, D.Q., Cheng, H., Duan, Q., Huang, W., 2015. Sodium houttuyfonate inhibits biofilm formation and alginate biosynthesis-associated gene expression in a clinical strain of Pseudomonas aeruginosa in vitro. Exp. Ther. Med. 10, 753–758. https://doi.org/10.3892/etm.2015.2562.